Solid-State High-Voltage Pulse Generator for Low Temperature Plasma Ion Mobility Spectrometry

Mohammad Ramezani, Amir Abbas Shayegani Akmal, and Kaveh Niayesh, *Senior Member, IEEE*

***Abstract*— Low-temperature plasma ion mobility spectrometry (LTP-IMS) is the method to identify some materials by measuring concentration of gas phase ions. IMS used in a wide range of laboratory-based biomedical research studies. A nanosecond pulse generator is necessary for LTP-IMS apparatus to enable direct analysis of various chemical compounds without having to evaporate the analyte or seek a solvent or any reagent. In this paper, a dual Marx pulsed generator for LTP-IMS Ionization power supply is proposed based on a new combination of some solid-state switches including insulated gate bipolar transistor (IGBT) and avalanche bipolar junction transistors (BJTs). The compact dual Marx generator is composed of a series of avalanche BJTs and an IGBT as the trigger switch, where its rise time is reduced from 100 to 5 ns by using an avalanche BJT in its command circuit. In this way, a controllable high-voltage pulse generator has designed, built, and tested. The proposed circuit can be used to generate the repetitive high-voltage pulses necessary for low temperature ionization in advanced IMS apparatus. The output voltage has an amplitude of up to 6 kV with pulse widths in the range of 40–1000 ns and pulse repetition rates up to 2 kHz, having rise time and fall time less than 10 ns independent of the load specifications.**

***Index Terms*— Avalanche bipolar junction transistor (BJT), dual Marx generator, low temperature plasma (LTP), solid-state switches.**

I. Introduction

PULSED power generators are used in many applications, with increasing demand in all kinds of industries, such as electrostatic precipitation [1], water treatment, plasma, pollution control [2], and detecting and identifying volatile, semivolatile organic compounds [3] as well as in medical and biological devices [4]–[6].

Ion mobility spectrometry (IMS) was developed over the past few decades as a method for detecting and identifying volatile and semivolatile organic compounds, principally in security and military venues. This technique is based on the determination of mobility in electric fields of gas phase ions derived from constituents in a sample [7].

Manuscript received May 13, 2018; revised October 3, 2018 and November 24, 2018; accepted January 19, 2019. The review of this paper was arranged by Senior Editor W. Jiang. *(Corresponding author: Amir Abbas Shayegani Akmal.)*

M. Ramezani and A. A. Shayegani Akmal are with the School of Electrical Engineering and Computer Engineering, University of Tehran, Tehran, Iran (e-mail: mo.ramezani@ut.ac.ir; shayegani@ut.ac.ir).

K. Niayesh is with the Department of Electric Power Engineering, Norwegian University of Science and Technology, Trondheim, Norway (e-mail: kaveh.niayesh@ntnu.no).

Color versions of one or more of the figures in this paper are available online at http://ieeexplore.ieee.org.

Digital Object Identifier 10.1109/TPS.2019.2894844

In this technique, the formation of gas phase ions precedes the process of ion separation and detection by mobility measurements. Ionization can occur after the evaporated sample enters the ionization or reaction region of the drift tube depending on the type of ion source used [8].

The ionization source is an important part of any ion mobility spectrometer that produces ions at ambient pressure. While investigations on the ion source for IMS date back a long time ago, research in this field has been revitalized due to its wide range of applications, especially in security, biological, and medical applications. Recently, low temperature plasma (LTP) was investigated as an ionization source for IMS, where pulsed generators are necessary for this application [9]. The LTP-IMS application requires short pulse rise time and high pulse repetition frequency (PRF) in order to maximize the efficiency [10].

In this paper, a compact Marx generator design is proposed to generate the necessary voltage pulses in a reliable and controllable manner. It is based on two-pulse circuits (a positive and a negative) using a combination of insulated gate bipolar transistor (IGBT) and avalanche bipolar junction transistors (BJTs). IGBTs are used as the main switch to achieve a better controlling of the output pulse, as they offer long lifetime and good stability in pulse modulator applications [11]. Avalanche transistor switches are utilized at all other stages of the Marx generator with regard to the benefits of fast switching speeds and high repetition frequencies [12].

A BJT-Marx generator circuit is widely used for generation of nanosecond high-voltage pulses due to its fast switching speed and high repetition frequency [13]. In previous studies, dual Marx generators are used for microplasma generation purposes [14].

The novelty of the proposed approach is using an avalanche BJT in the triggering circuitry of an IGBT in the dual Marx generator design to improve its switching performance and to reduce its turn-on time. In this way, fully controllable nanosecond output voltage pulses can be generated.

Based on this idea, a 6-kV pulse generator with an adjustable pulsewidth in the range of 40–1000 ns and a repetition rate of up to 2000 pulses per second, having rise time and fall time of each pulse less than 10 ns independent of the load is designed, built, and tested. The present pulse generator can be used to supply an LTP source for an ion mobility spectroscopy system. This pulse generator may also be employed to derive capacitive discharges such as dielectric barrier discharges where fast rising and falling times are desired.

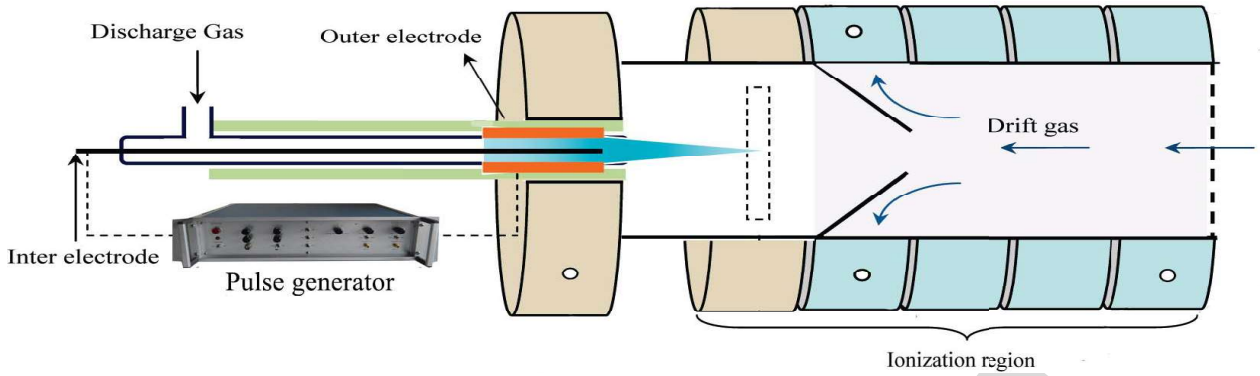

Fig. 1. Schematic of the desorption/ionization region for the LTP-IMS apparatus.

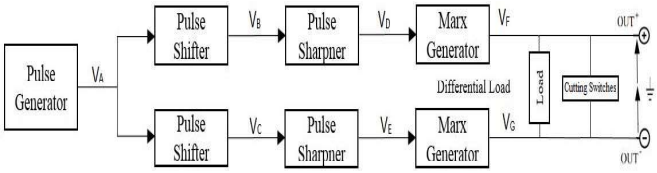

Fig. 2. Proposed block diagram for the high-voltage pulse generator.

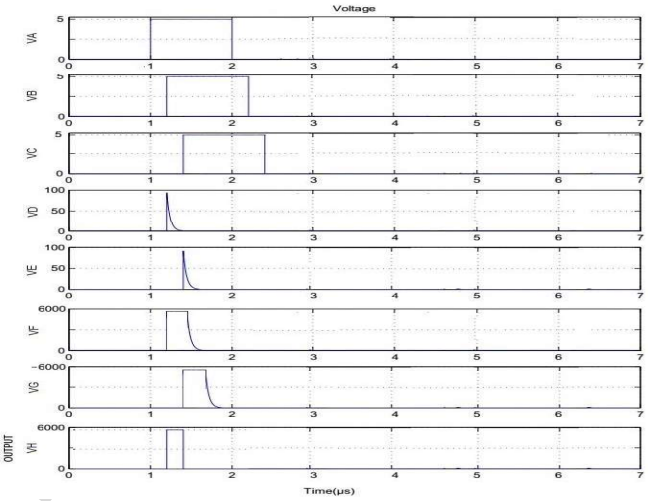

Fig. 3. Timing of the signals in the proposed method shown in Fig. 2. Pulse generator V_A, (V_B, V_C) are shifted pulse, (V_D, V_E) are Trigger Pulse for Marx generator, (V_F, V_G) Marx voltage, V_H is output voltage.

Experimental results showed that the designed dual solid states Marx generators can be used to apply higher voltage pulses with appropriate parameters, especially short fall times, to an LTP discharge in an ion mobility spectrometer.

II. Design of LTP-IMS Power Supply

A. Main Requirements of the Power Supply for LTP-IMS

An LTP-IMS apparatus consists of a nanosecond-kilovolt Marx generator as power supply and an LTP probe, as shown in Fig. 1. The LTP probe includes a glass tube and a stainless steel rod as the internal electrode, which is centered axially inside the glass tube. The drift gas enters the drift tube from behind the Faraday plate and flows toward the ionization/reaction region. The LTP-IMS pulse generators should generate high instantaneous power and low average power for producing LTP, the advantage of using this Marx pulse generator as power supply is controlling the LTP generation by regulation of the amplitude and pulsewidth of the output voltage [15]. One possibility is to keep the amplitude and the repetition rate constant (e.g., at 6 kV and 2000 pulses per second) and to control the ionization (plasma production) level by changing the pulsewidth in the range of 40–1000 ns [16].

The proposed block diagram for the pulse generator is shown in Fig. 2. The first block is a pulse generator, which produces a command signal. This command signal is then delayed using two pulse shifter blocks to enable the pulsewidth adjustment. Two pulse sharpener blocks make the necessary narrow pulses for the Marx generator blocks. The load is connected in differential mode between these two Marx generators.

The output of each main block of the pulse generator is shown in Fig. 3. The output pulse of the first block (V_A) is a 5-V signal with a pulsewidth in microsecond range. In the pulse shifter blocks, appropriate delay times depending on the desired output pulsewidth are applied (V_B, V_C), in pulse sharpener, these two pulses are converted to nanoseconds pulses with higher amplitude for Marx generator biasing (V_D, V_E). Finally, Marx generators produce the demanded kilovolt nanosecond pulses. In the design built and tested in this paper, each Marx generator has 20 stages and the avalanche BJTs with breakdown voltages of 300 V are used [17].

In order to drive a 6-kV output voltage for LTP Power supply, in addition to 20 avalanche BJTs, an IGBT is used as a triggerable switch in each Marx generator. This makes it possible to realize the necessary variable pulse widths in a reliable manner. By simply changing the number of stages, even higher amplitudes of the output pulse can be realized.

B. Dual Marx Compact Generator

The schematic of the proposed pulse Marx generator is shown in Fig. 4. Here, R1–R40 are the charging resistors; Z1–Z2 are the fast IGBTs for fast rising switches; S1–S20 and

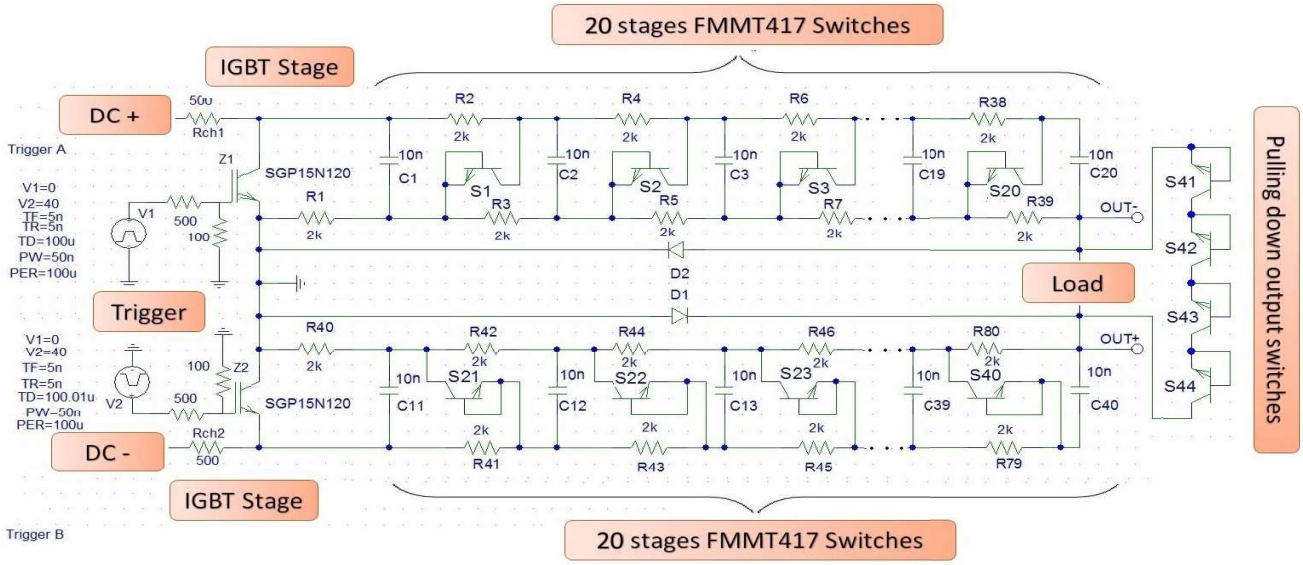

Fig. 4. Proposed circuit for the nanosecond-pulse generator.

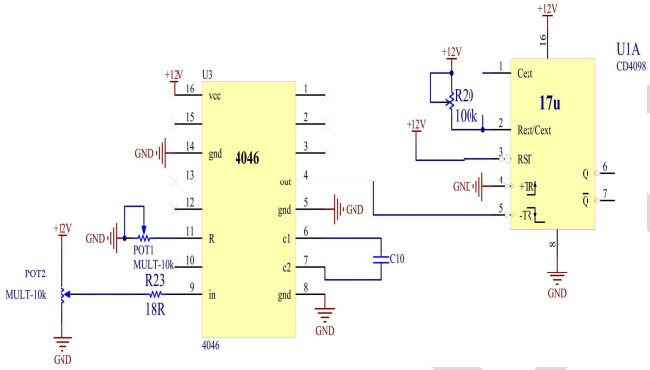

Fig. 5. Control pulses circuit used for IGBT fast triggering.

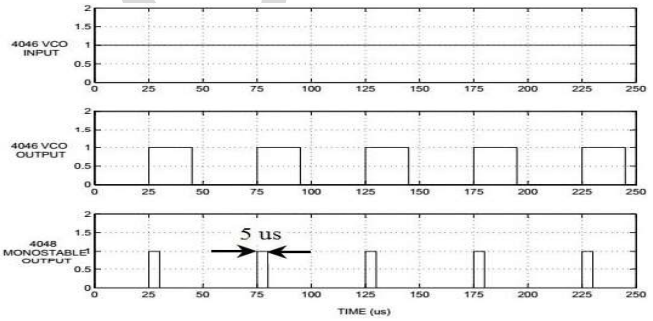

Fig. 6. Output pulse waveform from control pulse circuits.

S21–S40 are the avalanche BJT switches used as the main switches for two parallel Marx Generator, C1–C40 are the charging capacitors, and D1, D2 are the diodes for nonreturn voltage. The charging path for each circuit is provided by the charging resistors R1–R40 and capacitors (C1–C20). In charging mode, all capacitors are charged in parallel, the voltage of capacitor on each stage is equal to the value of the output voltage of the dc power supply. The capacitors on each stage are in series across the switches in the discharge cycle, and a positive pulse forms on the load with an amplitude of about $V\text{out} = n V\text{in}$ in the ideal case.

The main problem of using a Marx generator to generate nanosecond pulses is to reduce the pulse falling time, which should be comparable to the pulse rise time in LPT application.

A simple solution based on utilization of avalanche switches parallel to the load does not function practically as the uncontrolled high current flowing through the switches may damage them. Therefore, to avoid this, another Marx generator in combination with fast switches (S41–S44) can be used to pull down the output voltage within few nanoseconds to zero independent of the load. The number of these switches is related to the output pulse amplitude.

Avalanche transistor (FMMT417) has been used since a switching time of less than 5 ns at an applied voltage of 300–400 V is easily obtained [18]. In order to operate an IGBT for nanosecond switching applications, a fast pulse must be applied to the gate circuit of the IGBT. For this purpose, the output pulse of an avalanche BJT is applied to the gate of the fast IGBT. This enables turning on the IGBT very rapidly, which results in short rise time of the output voltage of the Marx generator. To take into account the electrical characteristic of the loads in LTP systems [19], the load has been modeled using a capacitance, an inductance, and a resistance, which is dependent of the phase gas ions. After ionization of the carrier gas, the load resistance is reduced resulting in an increased current flowing through the transistors. This may, in turn, lead to shortening the output voltage rise time and output voltage amplitude.

Hence, in the designed test circuit, appropriate measures have to be taken to choose the suitable stage capacitances in order to minimize the dependence of the output voltage on the load. The appropriate value for charging resistors is to be selected based on the required width of the output square-wave pulse. The power class of the charging resistors has to be chosen according to their maximum energy dissipation, which is proportional to the repetition rate.

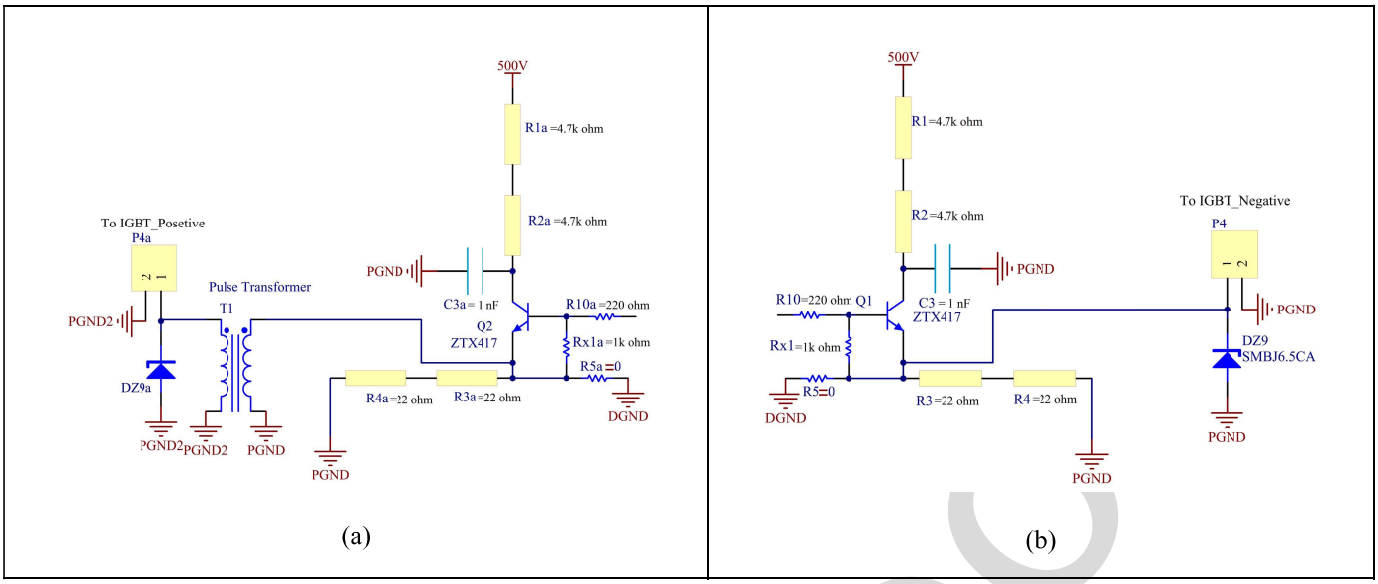

Fig. 7. IGBT gate driver used FMMT417 as a current source circuitry to turn on SGP15N120 IGBT easily and safe (a) for the positive pulser and (b) for the negative pulser.

C. Design of Control System and Driving Circuit

The excitation circuits are very important, in particular, for low-latency pulse generators. The circuits used in the propose design are shown in Fig. 5.

Initially, control pulses are produced by ICs 4046 and 4098. IC 4046 has an internal voltage-controlled oscillator. By changing the voltage in the control base, the output frequency changes. Output pulses are sent to the Mono-stable IC 4098. Mono-stable output pulsewidth is about 5 μs. The pulse waveform is shown in Fig. 6.

Here to drive IGBT fast, an avalanche transistor circuit is used as the gate driver to rapidly charge the larger input capacitance of the IGBT in order to turn it on within few nanoseconds (see Fig. 7). For this purpose, a high current pulse is injected into the gate of the IGBT to turn it on in a very short time. The details of this concept are discussed thoroughly in [18]. The FMMT417 avalanche transistors have a peak avalanche current of 60 A (pulsewidth = 20 ns), so using this switch in the driving circuit of SGP15N120 IGBT, will make it possible to turn it on easily.

The gate driver input signal and gate current is shown in Fig. 8. Driver voltage is about 120 V and The gate current is a pulse at about 8 A (measured using a 1-Ω resistance shunt) and with a rise time of 5 ns. This current, with very fast rise time, makes the IGBT turn on at a very high speed.

Since IGBT switches have different ground potentials in the positive and negative pulse generators, a pulse transformer [T1 in Fig. 7(a)] is used to isolate the ground potentials. The typical command trigger signals are shown in Fig. 9. The pulsewidth of the driving signal is about 1 μs, and both rise times are less than 20 ns. A small dead band between the rising edges of these two trigger signals corresponds to the width of the output voltage pulses.

To produce the necessary charging voltage of 500 V, a boost converter is built with TL494 IC as shown in Fig 10. This voltage is applied to the IGBT driver.

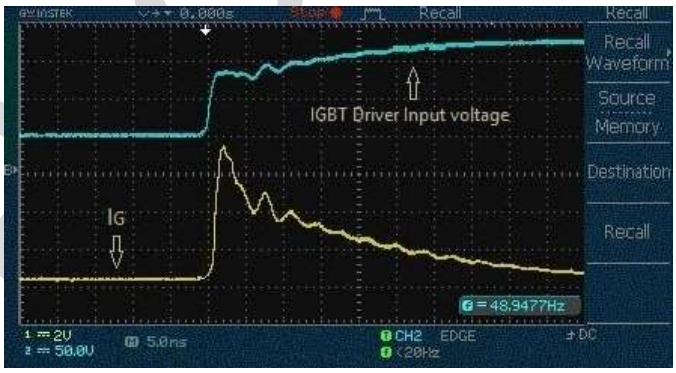

Fig. 8. Gate driver input signal and gate current on each avalanche transistor command circuits.

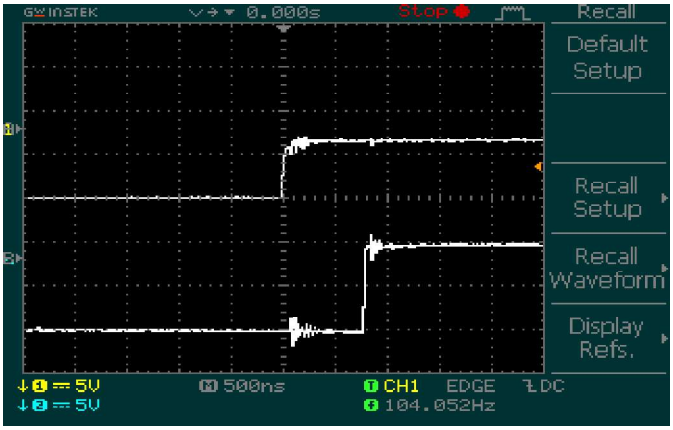

Fig. 9. Driving voltage waveforms of the main IGBT switches on each Marx generator circuits.

III. Simulation of Nanosecond-Pulse Generator

In this section, a 20 stage pulse generator of the proposed design is simulated. For this purpose, the IGBT model is selected from the Infineon database [20]. To be able to

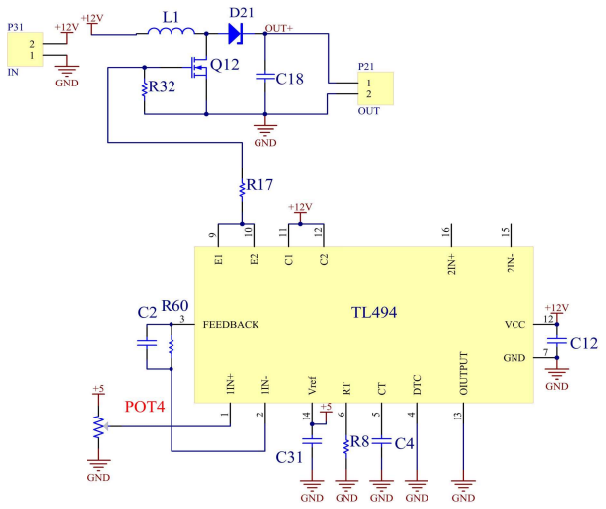

Fig. 10. High-voltage boost converter by TL494 IC.

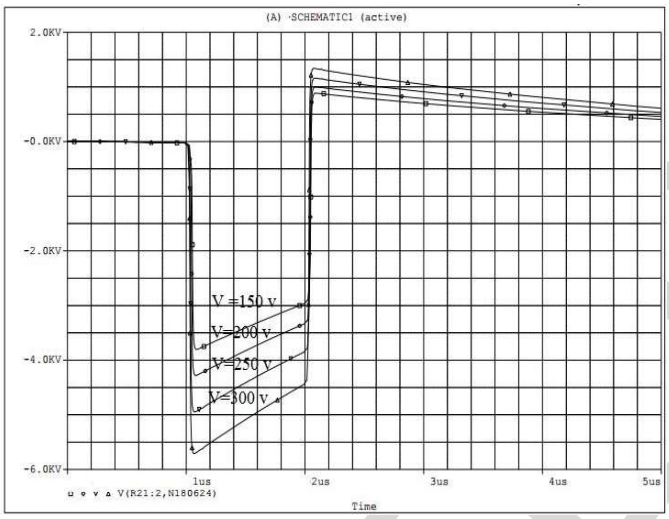

Fig. 11. Impact of the charging voltage on the voltage in case of pure resistance loads.

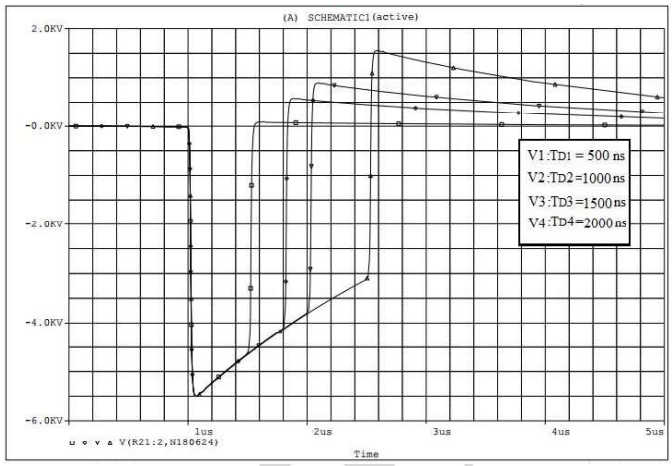

Fig. 12. Different pulse widths of the voltage waveforms.

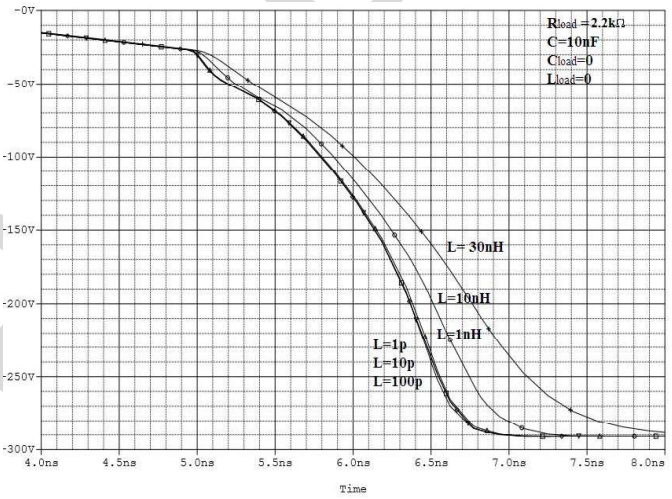

Fig. 13. Effect of stray inductance of the circuit on the output voltage.

model the avalanche breakdown phenomenon in avalanche BJTs, a generic model of bipolar transistors, namely, Gummel–Poon model, is extended using voltage-controlled switches, i.e., Zener diodes for generating the breakdown voltage, appropriate inductors and capacitors, as well as Schottky diodes for fast switching.

All charging capacitors and resistors are 10 nF and 5 KΩ, respectively. The load is modeled by a pure resistance, *RC* or *RL* combinations. For this application, the pulsewidth is in the range of 100 ns–1 μs and the PRF is 2 kHz. The influence of capacitance, turn-on delay time, and the stray inductance on the output voltage is investigated. The output waveforms for a pure resistive load are shown in Fig. 11. The output voltage amplitude is linearly proportional to the charging voltage of the capacitors.

In Fig 12, the pulse width is variable with constant input voltage and pure resistance, which used in this application. When ten modules of the generator are in series, the rise time of the positive HV pulse is about 20 ns and the fall time is few microseconds. In this simulation, pulsewidth of the waveform is varying from 500 to 2000 ns. Both rise and fall edges of the output waveforms are barely changed with the variation of pulse amplitude and pulsewidth.

By investigating the effect of the stray inductance on the breakdown voltage of the switch, it is concluded, as shown in Fig. 13, that in case of small stray inductances in the range of maximum few hundred pH, the rise time of the output voltage pulse does not change. This very low amount of the stray inductance can be achieved by a compact design of the circuits.

As mentioned, the ionization results in reduction of the load resistance. The impact of changing of the load resistance on the output voltage is shown in Fig. 14. A decreased load resistance increases the current passing through the transistors. Consequently, high currents are developed, the transistors break down faster, and the rise time of the output voltage is reduced. However, given the larger current flow, this results in reduction of the capacitor voltages. In case of very small loads (very high load resistances), the avalanche breakdown of switches do not occur and, therefore, the desired output pulse cannot be generated.

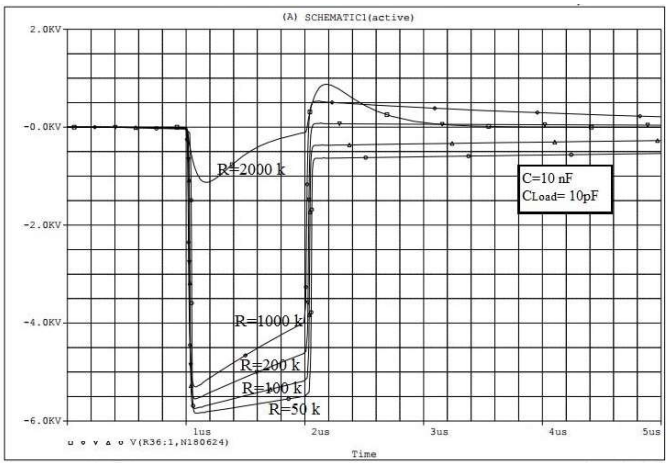

Fig. 14. Effect of the load resistance variation on the output voltage.

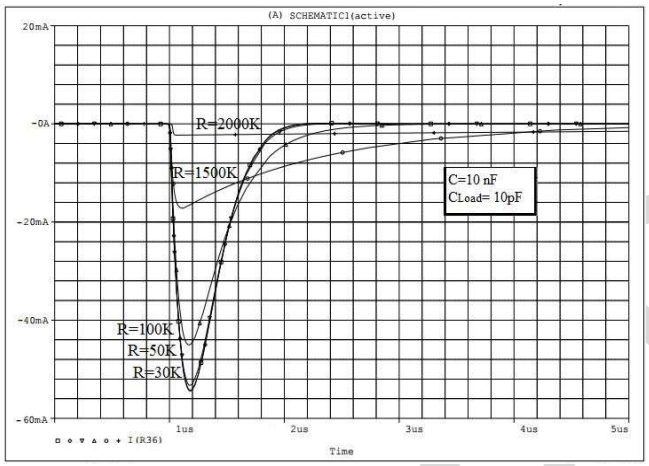

Fig. 15. Effect of the load resistance variation on the output current.

The increase in load (decrease in load resistance) will, in turn, results in very high current flowing through the switches. According to the datasheet of the switches, the maximum allowable current would be 60 A for pulses less than 20 ns. This means that minimum load resistance is dependent on the desired pulsewidth, e.g., for a pulsewidth of 1 μs, the minimum load resistance would be about 30 kΩ, corresponding to a peak current of 50 mA (see Fig. 15).

In Fig. 16, the output voltages for different stage capacitances have been modeled. In typical Marx generators, the load capacitance is near 1pF, which is much smaller than the charging capacitors. Therefore, the charging capacitance plays the main role in determination of falling and rising edge of the output pulse. Therefore, in the proposed model, the load capacitance can be ignored in both rise and fall time of the impulse voltage.

If a large capacitor used in this model, transistors lose the ability to break down and cannot supply the required power, very small capacitors, in contrast, do not significantly influence the output. The decreased amount of capacitors is expected to decrease the settling time of the output voltage.

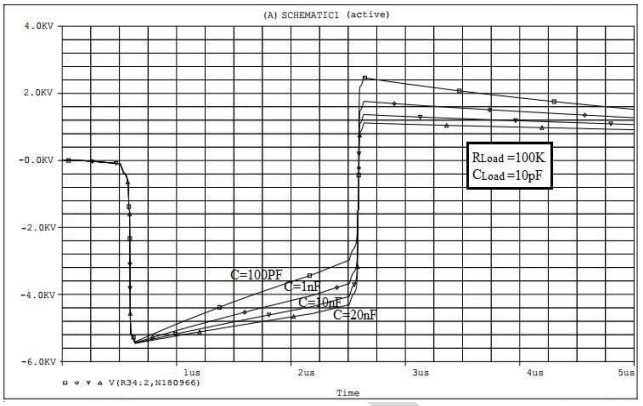

Fig. 16. Influence of the capacitance of the Marx stage capacitors on output waveform.

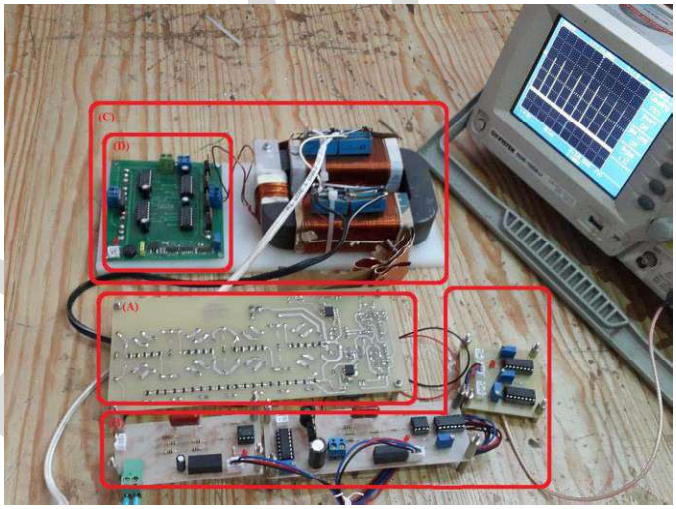

Fig. 17. Prototype of nanosecond-pulse power generator for LTP-IMS system main designed circuit for 6-kV pulse. (A) 20 stage of FMMT417 which each break down is 300-V Marx generator consist of capacitors and resistors. (B) Trigger circuit. (C) DC voltage supply. (D) DC voltage with 500-V output for IGBT drive.

IV. Test of Designed Generator

In this section, results of the tests performed on a 20-stage compact pulse generator of the proposed design are reported. The number of stages can be increased if higher output voltages are required. With increase in the number of stages, the current flowing through the transistors also increases. Therefore, the current ratings of the transistors may limit the maximum number of stages.

In the current design of the pulse generator, earth plates are utilized to decrease the stray inductances and for the purpose of noise suppression. They also provide the shortest path to the earth node all through the circuit, wherever necessary. In the actual testing process, charging voltage was adjusted continuously from 0 to 400 V by an autotransformer, waveforms are measured with an oscilloscope (GW Instec GDS-1000A-U Series Digital Storage Oscilloscopes) with the analog bandwidth being 200 MHz and the sampling rate of 2.5 GS/s.

Fig. 17 shows the designed nanosecond-pulse power generator for LTP-IMS system. The typical output voltage waveforms

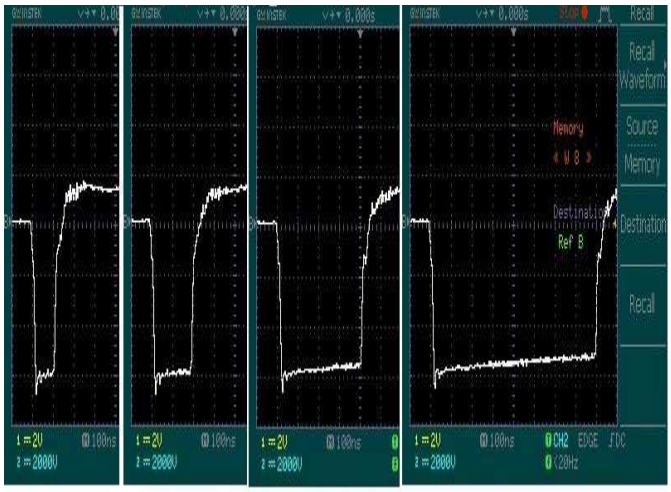

Fig. 18. Measured output voltage of the prototype pulse generator with different pulse widths between 50 ns and 1 μs.

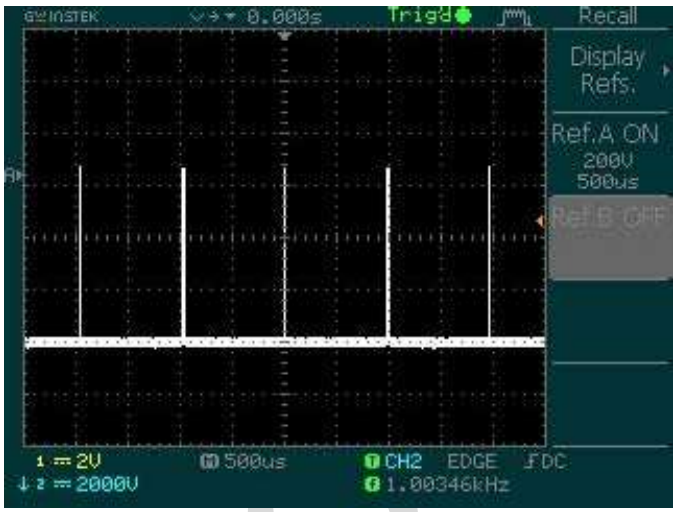

Fig. 19. Repetitive pulse applied to the LTP-IMS system with the repetition rate of 2 kHz.

with different pulse widths between 50 ns and 1 μs are shown in Fig. 18. The output voltage pulse has an amplitude of 6 kV at a PRF of 2 kHz.

For helium or argon, which are used as discharge gas in drift tube, the outer conductor diameter is 40 mm, inner conductor diameter is 21 mm, and the distance is near 80 mm so the load capacitance is near 1 pF.

Therefore, the choice of 10-nF capacitors for each stage seems to be appropriate. In this case, the generator's equivalent capacitance is equal to 500 pF, which is much larger than the load capacitance. For other applications, if a larger capacitor is selected for stages, it is possible to test larger loads. The voltage of the capacitor should be more than 250 V. In the built prototype, 10-nF 400-V capacitors have been used.

The charging resistances have been selected according to the requirement for the output square-wave pulse voltage

$$\tau = 5 \times n \times R_{\text{ch}} \times C_{\text{ch}} \tag{1}$$

where C_{ch} is the equivalent series capacitance, τ is the maximum pulsewidth, n is the number of stages, and R_{ch} is the charging resistance.

For the desired LTP-IMS system with a repetition rate of 2 KHz, maximum charging time of the capacitors is 500 μs, so the maximum charging resistor will be 5 kΩ according to (1).

The required power level of the resistors is selected based on the energy dissipation by one discharge and the repetition rate. For the current design of the generator, the power dissipation of each charging resistor is about 0.4 W.

According to the proposed design, the PRF of the nanosecond pulse generator can be adjusted between 100 Hz and 2 kHz. Fig. 19 shows the applied voltage has an amplitude of 6 kV, the pulsewidth of about 250 ns at a PRF of 2 kHz.

Fig. 20 shows the typical voltage–current waveform and discharge image of LTP Ion mobility system. The applied voltage amplitude is about 6 kV, the pulsewidth is about 550 ns, PRF is 2 kHz, and gas-flow rate is about 0.5 L/min. The load current measured using a 1-Ω resistance shunt.

Fig. 20. Typical voltage–current waveform image of LTP Ion mobility system.

The discharge of the LTP Ion mobility system generated by nanosecond-pulse generator is very stable. Given that the rise/fall time of the applied nanosecond pulse is fast, two remarkable current pulses can be measured at both the rise and fall edges.

The discharge currents are below 200 mA, and the negative discharge current is lightly larger than the positive discharge current. The positive polarity discharge begins at the rising edge, and when the applied voltage reaches the peak value, the discharge current reaches its maximum. However, the negative polarity discharge begins at the falling edge of the pulse and reaches the maximum value after the applied voltage becomes zero According to the analysis, the negative discharge is generated by the charge accumulated in the strong electric field during positive polarity discharge, which ionizes the analyte molecules.

V. Conclusion

A compact nanosecond-kilovolt pulsed power supply with solid-state switches has been developed for LTP-IMS

systems. In this design, a reverse Marx generator is used to truncate the output voltage, and in this way, to control the parameters of the output pulse. For this purpose, the trigger signals of the main switches are controlled by fast oscillating circuitries. Based on the simulation results, a 20-stage Marx generator using avalanche BJTs and IGBTs has been designed, constructed, and tested. The pulse amplitude, pulsewidth, and repetition frequency, can be freely adjusted in the range of 0–10 kV; 40–1000 ns; 1–2 kHz, enabling detection of different materials in the LTP IMS applications.

Test results performed on a 20-stage prototype show that a stable 6-kV square wave pulse series with a rise time of 20 ns and a fall time of ∼25 ns can be generated, where the pulsewidth and repetition frequency can be freely adjusted. The limiting factor of the maximum voltage and pulsewidth in such Marx generators has been identified as the most important feature of the proposed design.

REFERENCES

[1] M. Takasaki, H. Kurita, K. Takashima, M. Hayashi, A. Mizuno, and T. Kubota, "Electrostatic precipitation of diesel PM at reduced gas temperature," in *Proc. IEEE Ind. Appl. Soc. Annu. Meeting*, Oct. 2015, pp. 1–4.

[2] Z. Li *et al.*, "The effects of pulsed streamerlike discharge on cyanobacteria cells," *IEEE Trans. Plasma Sci.*, vol. 34, no. 5, pp. 1719–1724, Oct. 2006.

[3] H. Akiyama, T. Sakugawa, K. Takaki, Y. Minamitani, N. Shimomura, and T. Namihira, "Industrial applications of pulsed power technology," *IEEE Trans. Dielectr. Electr. Insul.*, vol. 14, no. 5, pp. 1051–1064, Oct. 2007.

[4] Y. Li, M. Ying, M. H. Kang, H. S. Uhm, J. Lee, E. H. Choi, and I. Han, "Effects of atmospheric-pressure non-thermal bio-compatible plasma and plasma activated nitric oxide water on cervical cancer cells," *Sci. Rep.*, vol. 7, Mar. 2017, Art. no. 45781.

[5] M. Ishaq, M. Evans, and K. Ostrikov, "Effect of atmospheric gas plasmas on cancer cell signaling," *Int. J. Cancer*, vol. 134, no. 7, pp. 1517–1528, 2014.

[6] X. Lu, G. V. Naidis, M. Laroussi, S. Reuter, D. B. Graves, and K. Ostrikov, "Reactive species in non-equilibrium atmospheric-pressure plasmas: Generation, transport, and biological effects," *Phys. Rep.*, vol. 630, pp. 1–84, May 2016.

[7] H. Akiyama, S. Sakai, T. Sakugawa, and T. Namihira, "Invited paper—Environmental applications of repetitive pulsed power," *IEEE Trans. Dielectr. Electr. Insul.*, vol. 14, no. 4, pp. 825–833, Aug. 2007.

[8] H. Borsdorf and G. A. Eiceman, "Ion mobility spectrometry: Principles and applications," *Appl. Spectrosc. Rev.*, vol. 41, no. 4, pp. 323–375, 2007.

[9] G. Eiceman, Z. Karpas, and H. H. Hill, *Ion Mobility Spectrometry*, 3rd ed. Boca Raton, FL, USA: CRC Press, 2013.

[10] C. Uetrecht, R. J. Rose, K. Lorenzen, A. J. R. Heck, and E. van Duijn, "Ion mobility mass spectrometry of proteins and proteinassemblies," *Chem. Soc. Rev.*, vol. 39, no. 5, pp. 1633–1655, 2010.

[11] X. Lu, G. V. Naidis, M. Laroussi, and K. Ostrikov, "Guided ionization waves: Theory and experiments," *Phys. Rep.*, vol. 540, no. 3, pp. 123–166, 2014.

[12] W. Ding, Y. Wang, C. Fan, Y. Gou, Z. Xu, and L. Yang, "A subnanosecond jitter trigger generator utilizing trigatron switch and avalanche transistor circuit," *IEEE Trans. Plasma Sci.*, vol. 43, no. 4, pp. 1054–1062, Apr. 2015.

[13] Z. Li, P. Li, S. Jiang, T. Sakugawa, and J. Rao, "Theoretical analysis and improvement on pulse generator using BJTs as switches," *IEEE Trans. Plasma Sci.*, vol. 44, no. 10, pp. 2053–2059, Oct. 2016.

[14] T. Heeren, T. Ueno, D. Wang, T. Namihira, S. Katsuki, and H. Akiyama, "Novel dual Marx generator for microplasma applications," *IEEE Trans. Plasma Sci.*, vol. 33, no. 4, pp. 1205–1209, Aug. 2005.

[15] M. T. Jafari, "Low-temperature plasma ionization ion mobility spectrometry," *Anal. Chem.*, vol. 83, no. 3, pp. 797–803, 2010.

[16] X. Lu *et al.*, "A cold plasma cross made of three bullet-like plasma plumes," *Thin Solid Films*, vol. 518, no. 3, pp. 967–970, 2009.

[17] S. Dong, C. Yao, T. Luo, Y. Zhou, C. Wang, and N. Yang, "Solid-state nanosecond-pulse plasma jet apparatus based on Marx structure with crowbar switches," *IEEE Trans. Plasma Sci.*, vol. 44, no. 12, pp. 3353–3360, Dec. 2016.

[18] N. S. B. Othman, T. Jindo, M. Yamada, M. Tsuyama, and H. Nakano, "Fast high voltage solid state switch using insulated gate bipolar transistor for discharge-pumped lasers," *World Acad. Sci., Eng. Technol., Int. J. Elect., Comput., Energetic, Electron. Commun. Eng.*, vol. 8, no. 12, pp. 1869–1872, 2014. AQ:4

[19] S. Nguyen-Kuok, "The theoretical basis of the low-temperature plasma," in *Theory of Low-Temperature Plasma Physics*. Cham, Switzerland: Springer, 2017, pp. 1–51.

[20] [Online]. Available: https://www.infineon.com/cms/en/tools/solution-finder/product-finder/simulation-model AQ:5

Mohammad Ramezani received the B.Sc. and M.Sc. degrees in electrical engineering from the Amirkabir University of Technology, Tehran, Iran, in 2011 and 2013, respectively, where he is currently pursuing the Ph.D. degree in electrical engineering.

His current research interests include pulsed power technology and plasma modeling.

Amir Abbas Shayegani Akmal received the B.Sc. degree in power engineering from the Sharif University of Technology, Tehran, Iran, in 1996, and the M.Sc. and Ph.D. degrees in power engineering from the University of Tehran, Tehran, in 1998 and 2005, respectively, the Ph.D. degree in electrical engineering from the University of Tehran, with the cooperation of the Schering-Institute, University of Hannover, Hannover, Germany.

He is currently a Faculty Member with the School of Electrical and Computer Engineering, University of Tehran. His current research interests include high-voltage insulation systems, testing, and diagnostics.

Kaveh Niayesh (S'98–M'01–SM'08) received the B.Sc. and M.Sc. degrees in electrical engineering from the University of Tehran, Tehran, Iran, in 1993 and 1996, respectively, and the Ph.D. degree in electrical engineering from the RWTH-Aachen University of Technology, Aachen, Germany, in 2001.

He held different academic and industrial positions including a Principal Scientist with the ABB Corporate Research Center, Baden-Dättwil, Switzerland; an Associate Professor with the University of Tehran; and the Manager of basic research with AREVA T&D, Regensburg, Germany. He is currently a Professor with the Department of Electric Power Engineering, Norwegian University of Science and Technology, Trondheim, Norway. He has authored or co-authored over 110 journal and conference papers on current interruption and limitation, vacuum and gaseous discharges, plasma modeling and diagnostics, switching transients, and pulsed power technology.